Zero : Jurnal Sains, Matematika, dan Terapan
E-ISSN : 2580-5754; P-ISSN : 2580-569X
Volume 10, Number 2, 2026
DOI: 10.30829/zero.v10i2.29891
Page: 602-613

Delay Tolerance and Recovery Control in a Synchronized Electric Bus Network using Max-Plus Algebra

[1]Marcellinus Andy Rudhito
Department of Mathematics Education, Sanata Dharma University, Yogyakarta, 55281, Indonesia

[2]Dewa Putu Wiadnyana Putra
Department of Mathematics Education, Sanata Dharma University, Yogyakarta, 55281, Indonesia

Article Info

Article history:

Accepted: 10 July 2026

Keywords:
Delay Tolerance;
Electric Bus Network;
Max-Plus Algebra;
Recovery Control;
Switching Policy.

ABSTRACT

This study analyzed delay tolerance, normalization time, and recovery control in the two-terminal Trans Gadjah Mada Electric Bus network using max-plus algebra. An analytical-computational approach was applied by representing the nominal route times as a weighted directed graph and transforming them into a max-plus linear system. The max-plus eigenvalue, critical arcs, component-wise delay thresholds, excess delays, and recovery horizons were then computed. The nominal synchronized period was 21 minutes. The Terminal 1 and Terminal 2 local routes had delay thresholds of 2 and 3 minutes, respectively, whereas both interterminal corridors were critical arcs with zero delay tolerance. Thus, any positive delay on a critical corridor directly disturbed synchronization. Service-operational delays changed route weights, while departure-time delays shifted terminal event times. The resulting threshold and excess-delay measures provided the mathematical basis for a simple recovery-mode switching rule, whose parameters remain illustrative and require empirical calibration before operational deployment.

Corresponding Author:

Marcellinus Andy Rudhito,
Department of Mathematics Education,
Sanata Dharma University, Yogyakarta, Indonesia
Email: rudhito@usd.ac.id

1. INTRODUCTION

The Trans Gadjah Mada Electric Bus (TGMEB) is a campus electric-bus service that requires synchronized departures between terminals. A previous route-design study indicated that a two-terminal configuration is an efficient alternative with a service period of 21 minutes [1]. That result provides a basis for the nominal timetable, but it does not yet explain how the timetable responds when a delay occurs either at departure or during service operation.

A synchronized transportation service can be viewed as a discrete-event system because its main variables are event times, such as departures, arrivals, and vehicle releases from terminals. In such a system, a departure often has to wait until several preceding events have been completed. The maximum operation is therefore natural for representing synchronization, whereas ordinary addition represents travel time or processing time. Max-plus algebra provides a framework for modeling such synchronized systems [2–4] . The discrete-event-system perspective also emphasizes the importance of event ordering and release rules in transportation systems [5].

In actual operations, delays may arise from two different sources. First, a departure-time delay occurs when a bus cannot depart at its planned time, for example because the driver is not yet ready, passengers are still boarding, or the terminal cannot yet release the bus. Second, a service-operational-time delay occurs when the travel time of a route exceeds its nominal value, for example because of traffic congestion, intersection conflicts, rain, access restrictions, or charging-related needs. These two types of delay may appear similar in the arrival clock time, but they enter the model at different points: a departure delay shifts the event time $x_j(k)$, whereas a service-operational delay changes the route weight a_{ij}

Recent max-plus studies have continued to show the relevance of max-plus algebra for synchronized discrete-event systems. Railway and scheduling studies have used max-plus automata and Kleene-star-based methods to compress timetables, construct scheduling interfaces, and support time-triggered services [6–8]. Max-plus control and optimization studies have also addressed global optimization, approximate optimal control, interval systems, switched max-plus linear-dual inequalities, and production scheduling [9–11]. These studies indicate that max-plus models are suitable for representing event synchronization, mode changes, and recovery decisions in systems whose next state depends on the latest preceding event [12, 13].

Recent electric-bus studies have emphasized planning, vehicle scheduling, charging scheduling, and timetable feasibility. Reviews of electric-bus planning and charging scheduling show that battery capacity, charging strategy, route schedule, and charging infrastructure must be considered jointly [14, 15]. Other studies have modeled stochastic travel time, stochastic energy consumption, capacitated charging stations, and flexible timetable shifting to improve the reliability of electric-bus operation [16–18]. Charging-schedule optimization has also considered time-of-use electricity prices, time-of-day tariffs, multi-port charging stations, and opportunity-charging delay propagation [19–21]. Opportunity-charging models further show how charging delays may propagate into electric-bus departures [22].

Further electric-bus studies show that charging prices, charger capacity, energy consumption, and battery loss strongly affect operational feasibility [23–25]. Replacement strategies are also relevant because they connect charging decisions with operational recovery when energy and schedule constraints interact [26]. Charging-infrastructure reviews and optimization models emphasize the importance of matching charging technology, energy-storage support, and opportunity fast charging with daily bus operations [27–29]. Range uncertainty also needs to be considered because it affects route planning, charging needs, and schedule reliability [30].

However, these studies mostly address fleet-scale scheduling, charging optimization, infrastructure planning, or general max-plus formulations. They do not explicitly formulate component-wise delay tolerance, excess-delay propagation, normalization time, and recovery-mode switching within a small synchronized two-terminal campus electric-bus network. Therefore, the mathematical gap addressed in this study is not route design or fleet-scale charging optimization, but the characterization of how local and critical route components respond differently to delay in a max-plus synchronized network.

Based on this gap, this study aims to analyze delay thresholds, normalization time, and recovery switching in the two-terminal TGMEB network using max-plus algebra. The previous study of TGMEB established the nominal two-terminal route configuration and synchronized service period, whereas this study analyzes the response of that nominal structure to delay. The contribution of this article is twofold. Mathematically, it links the critical arcs, component-wise delay thresholds, excess-delay propagation, normalization horizons, and recovery-mode switching in one max-plus analytical framework. Operationally, it interprets these mathematical indicators as a simple basis for distinguishing normal operation, local recovery, and fast-mode recovery. Thus, the proposed switching rule is not presented as a final empirical control policy, but as an analytical consequence of the max-plus delay-tolerance structure.

2. RESEARCH METHOD

This study was designed as an analytical-computational study based on the two-terminal Trans Gadjah Mada Electric Bus (TGMEB) network reported in the previous route-design study [1]. The object of analysis was not a new network construction, but the selected two-terminal configuration, in which Terminal 1 is located at AT/FMIPA and Terminal 2 is located at AA/GSP. The data source consisted of nominal operational times from the previous model: 19 minutes for the Terminal 1 local route, 18 minutes for the Terminal 2 local route, and 21 minutes for each interterminal corridor [1]. These values were treated as deterministic route weights in the max-plus model.

The use of deterministic route weights in this study was intentional. The purpose of the analysis was to examine the structural synchronization properties of the nominal two-terminal network before introducing stochastic variability. In the max-plus framework, deterministic weights make it possible to identify the nominal eigenvalue, critical arcs, and delay thresholds in a transparent way. Therefore, the nominal operational times of 19, 18, and 21 minutes were treated as baseline weights rather than as daily operational averages estimated from field observations. This modeling choice allowed the study to isolate the mathematical effect of delay on synchronization.

The analysis was conducted through six stages. First, the two-terminal network was represented as a weighted directed graph, where each arc weight denotes the nominal service time or travel time of the corresponding route component. Second, the weighted graph was transformed into a max-plus linear model, in which the maximum operation represents synchronization among event times and ordinary addition represents the accumulation of travel or service time. Third, the nominal model was analyzed by determining the max-plus eigenvalue, eigenvector, and critical components. The initial state is chosen as an eigenvector, ensuring that the system exhibits periodic behavior from the outset. Fourth, the delay-absorption capacity of each component was computed by comparing its nominal operational time with the synchronized period. Fifth, the disturbance analysis was separated into service-operational-time delay and departure-time delay. Sixth, the excess-delay indicators were used to estimate the normalization horizon and to formulate a switching policy for normal, local-recovery, and fast modes recovery.

The parameters used in the recovery analysis, including setup cost, recovery rate, predictive horizon, and hysteresis margin, were treated as illustrative parameters. They were not estimated from GPS records, passenger-demand data, charging logs, or daily delay observations. A scenario-based sensitivity check was used to examine whether the classification of absorbed delay, excess delay, and recovery mode remained consistent when the disturbance location, disturbance magnitude, recovery rate, setup cost, and predictive horizon were varied. Their role was to demonstrate how the excess-delay indicators obtained from the max-plus model can be connected to a switching decision. The switching policy adopted in this study is based on a theoretical heuristic framework. The calibration of its parameters requires further validation against empirical data. Consequently, the proposed recovery rule should be interpreted as an initial analytical heuristic rather than as a final empirical control policy. Empirical calibration is still required before the rule can be implemented in actual TGMEB operations.

This study did not use direct field observations, GPS tracking records, passenger-demand data, or actual daily delay logs. Therefore, the results should not be interpreted as a final empirical evaluation of TGMEB operations. Instead, the study provides an analytical framework that can be used as a basis for field-data calibration and operational testing. To strengthen internal consistency, the model was checked through numerical disturbance scenarios involving local-route delays, interterminal-corridor delays, departure-time delays, and different recovery horizons. These scenarios function as computational verification of the proposed thresholds and switching rules. Further empirical validation should be conducted by collecting actual departure times, travel times, charging-related delays, and passenger-demand patterns from daily TGMEB operations.

The deterministic model used in this study can be extended to stochastic or uncertain settings by replacing fixed route weights with interval-valued or random max-plus weights. In such an extension, the max-plus update rule remains valid for each realized sample path because synchronization still depends on the latest completed predecessor event. However, the recovery horizon would no longer be interpreted only as a deterministic value. It could be evaluated as a worst-case bound, an expected recovery time, or a quantile-based recovery horizon under probabilistic delay assumptions. Correlated disturbances, such as congestion affecting both interterminal corridors, would require joint delay scenarios or stochastic simulations. These extensions are outside the scope of the present deterministic baseline model and are proposed as future empirical and computational work.

No human participants, animals, or personal data were involved in this study. Therefore, ethical approval was not required. The study was limited to mathematical modeling, analytical computation, and numerical scenario verification based on previously reported nominal route-time data.

3. RESULT AND ANALYSIS

3.1 Two-Terminal Network and Model Construction

Figure 1 shows the synchronization scheme of the two-terminal TGMEB network. The figure is not a geographic map but a weighted graph indicating time relations between terminal events. The AT node denotes Terminal 1 and the AA node denotes Terminal 2. The loop arc at AT denotes the Terminal 1 local route with a duration of 19 minutes, whereas the loop arc at AA denotes the Terminal 2 local route with a duration of 18 minutes. The two interterminal arcs denote the AT–AA and AA–AT corridors, each with a duration of 21 minutes.

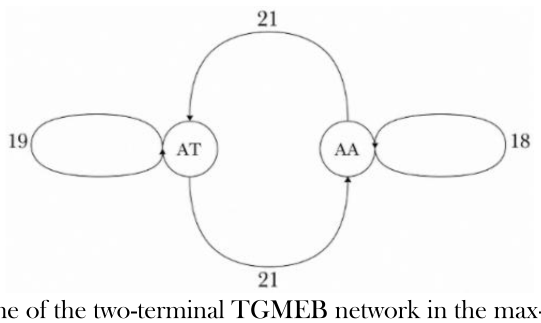

Figure 1. Scheme of the two-terminal TGMEB network in the max-plus model [1].

Let $x_1(k)$ denote the departure time of Terminal 1 in cycle k and $x_2(k)$ denote the departure time of Terminal 2 in cycle k. If a_{ij} denotes the time from the event at terminal j to the event at terminal i, then the next departure at terminal i must wait for all relevant inputs. With operations $a \oplus b = max(a,b)$ and $a \otimes b = a + b$, this relation is written as the max-plus linear system.

$$x(k+1) = A \otimes x(k), \tag{1}$$

or, component wise,

$$x_i(k+1) = \max_j\{a_{ij} + x_j(k)\}. \tag{2}$$

For the two-terminal TGMEB case, the nominal weight matrix is

$$A = \begin{bmatrix} 19 & 21 \\ 21 & 18 \end{bmatrix}. \tag{3}$$

Thus,

$$\begin{bmatrix} x_1(k+1) \\ x_2(k+1) \end{bmatrix} = \begin{bmatrix} 19 & 21 \\ 21 & 18 \end{bmatrix} \otimes \begin{bmatrix} x_1(k) \\ x_2(k) \end{bmatrix}. \tag{4}$$

The max-plus eigenvalue λ and eigenvector v satisfy

$$A \otimes v = \lambda \otimes v. \tag{5}$$

For matrix (3), $\lambda = 21$ minutes and $v = (0,0)^T$. In max-plus algebra, an eigenvector is determined up to an additive scalar; therefore, the general form of eigenvector of equation (5) is $v = (a,a)^T$ where $a \in \mathbb{R}$. Physically, adding the same scalar to both components of the eigenvector only shifts the common time origin of the two terminals. It does not change the relative synchronization phase between Terminal 1 and Terminal 2. For the sake of computational simplicity, the eigenvector is taken to be $v = (0,0)^T$.

Eigenvalue $\lambda = 21$ means that the nominal synchronized timetable can be constructed with a 21-minute period and both terminals have the same departure phase. The two interterminal corridors have weights equal to the nominal period and therefore form critical components. By contrast, the two local routes have weights smaller than 21 minutes and consequently have delay-absorption capacity. The imbalance between the local route times 19 and 18 minutes and the synchronized period 21 minutes is reflected in the delay thresholds of the non-critical loops, rather than in different eigenvector components.

Table 1. Nominal route components in the two-terminal max-plus model

Matrix entry	Operational interpretation	Nominal time (minutes)	Critical status
$\boldsymbol{a_{11}}$	Terminal 1 local route (AT to AT)	19	Non-critical
$\boldsymbol{a_{12}}$	Interterminal connection from Terminal 2 to Terminal 1	21	Critical
$\boldsymbol{a_{21}}$	Interterminal connection from Terminal 1 to Terminal 2	21	Critical
$\boldsymbol{a_{22}}$	Terminal 2 local route (AA to AA)	18	Non-critical

3.2 Service-Operational-Time Delay

A service-operational-time delay occurs when a route requires more time than its nominal weight. If the route from terminal j to terminal i has delay $d \geq 0$, then the weight a_{ij} becomes $a_{ij} + d$ in that cycle. For the timetable to remain within the nominal synchronization bound, the component must not exceed the eigen-relation. From Equation (5), the delay threshold is obtained as

$$\theta_{ij} = \lambda + v_i - v_j - a_{ij}. \tag{6}$$

Since $v_1 = v_2 = 0$ in this case, the formula becomes

$$\theta_{ij} = 21 - a_{ij}. \tag{7}$$

If the actual delay is d, the portion of delay that cannot be absorbed by the nominal timetable is expressed as

$$D_{ij}(d) = max\{0, d - \theta_{ij}\}. \tag{8}$$

The value $D_{ij}(d) = 0$ means that the operational delay is still absorbed. The value $D_{ij}(d) > 0$ means that there is excess delay that may shift the next departure.

Table 2. Service-operational delay thresholds in the two-terminal TGMEB model

Matrix entry	Route component	a_{ij}	$\theta_{ij} = 21 - a_{ij}$	Interpretation
a_{11}	Terminal 1 local route	19	2	Delays up to 2 minutes are absorbed
a_{12}	Terminal 2 to Terminal 1	21	0	Any delay affects synchronization
a_{21}	Terminal 1 to Terminal 2	21	0	Any delay affects synchronization
a_{22}	Terminal 2 local route	18	3	Delays up to 3 minutes are absorbed

Table 2 shows the different roles of local routes and interterminal routes. The Terminal 1 local route can absorb operational delay of up to 2 minutes, whereas the Terminal 2 local route can absorb operational delay of up to 3 minutes. The two interterminal routes have no absorption space because both are critical components. Consequently, any positive operational delay on an interterminal corridor becomes excess delay.

To clarify the use of the threshold in Equation (8), suppose that the normalized initial condition in a cycle is $x_1(k) = x_2(k) = 0$. Suppose some cases of experiences an additional service time $d = 1$ for Terminal 1 local route $(O1)$, $d = 5$ for Terminal 1 local route $(O2)$, $d = 5$ for Terminal 2 local route $(O3)$, and $d = 2$ for Terminal 2 corridor $(O4)$. Table 3 gives the summary of numerical computation of excess delay and the interpretation of the synchronized system.

Table 3. Numerical examples of service-operational-time delay

Case	Disturbed component	Additional time d	Threshold θ_{ij}	Excess D_{ij}	Interpretation
O1	Terminal 1 local route (a_{11})	1	2	0	Absorbed by the timetable
O2	Terminal 1 local route (a_{11})	5	2	3	Requires recovery due to a 3-minute deviation
O3	Terminal 2 local route (a_{22})	5	3	2	Requires recovery due to a 2-minute deviation
O4	Terminal 1 to Terminal 2 corridor (a_{21})	2	0	2	Immediately disturbs synchronization

3.3 Departure-Time Delay

Departure-time delay differs from operational delay because the disturbance does not appear in the route weight, but in the terminal event time. Suppose that the departure from terminal j in cycle k is delayed by $\delta_j(k)$. Then the time used in the update becomes $x_j(k) + \delta_j(k)$. For a destination terminal i, its effect can be read from

$$x_i(k+1) = \max_j\{a_{ij} + x_j(k) + \delta_j(k)\}. \tag{9}$$

If only one departure at terminal j is delayed by δ, the excess delay on relation $j \rightarrow i$ has the same form as Equation (8), namely

$$\Delta_{ij}(\delta) = \max\{0, \delta - \theta_{ij}\}. \tag{10}$$

The difference lies in the interpretation. In operational delay, d represents additional travel time on a route. In departure-time delay, δ represents a shift in the bus release time from the terminal. Both may produce the same excess delay, but the operational interventions are different. Operational delay can be handled through route or travel-time management, whereas departure delay is more closely related to terminal discipline, fleet readiness, and release rules.

Table 4. Impact of departure-time delay on subsequent relations

Delayed departure	Affected relation	Threshold	Initial impact
Terminal 1	Terminal 1 to Terminal 1 (a_{11})	2 minutes	Absorbed if $\delta \leq 2$
Terminal 1	Terminal 1 to Terminal 2 (a_{21})	0 minutes	Every $\delta > 0$ shifts Terminal 2
Terminal 2	Terminal 2 to Terminal 1 (a_{12})	0 minutes	Every $\delta > 0$ shifts Terminal 1
Terminal 2	Terminal 2 to Terminal 2 (a_{22})	3 minutes	Absorbed if $\delta \leq 3$

Table 4 shows that a departure delay from Terminal 1 is immediately critical when it affects the corridor to Terminal 2, whereas a departure delay from Terminal 2 is immediately critical when it affects the corridor to Terminal 1. Thus, release-time discipline at the two main terminals is as important as corridor travel-time control. In actual operation, this information can be translated into monitoring priorities: small delays in interterminal bus release should be recorded immediately, whereas small delays on local loops can still be tolerated as long as they do not exceed the threshold.

Suppose that the initial condition in a cycle is $x_1(k) = x_2(k) = 0$. By applying computation on (9), if the departure from Terminal 1 is delayed by $\delta_1 = 3$ minutes, then

$$x_1(k+1) = max\{19+3, 21\} = 22, \tag{11}$$

and

$$x_2(k+1) = max\{21+3, 18\} = 24. \tag{12}$$

Compared with the 21-minute nominal timetable, the normalized deviation becomes $z(k+1) = (1,3)^T$. The 1-minute deviation at Terminal 1 appears because the Terminal 1 local loop still has a 2-minute threshold, whereas the 3-minute deviation at Terminal 2 appears because the Terminal 1 to Terminal 2 corridor has a zero threshold.

A similar computational procedure was performed for the case of $\delta_1 = 1$ at Terminal 1 and $\delta_2 = 4$ at Terminal 2. The resulting computations and their implications for departure deviations are summarized in Table 5.

Table 5. Numerical examples of departure-time delay

Case	Delayed departure	Delay magnitude	Normalized deviation in the next cycle	Implication
K1	Terminal 1	$\delta_1 = 1$	$(0,1)^T$	The corridor to Terminal 2 begins to be disturbed
K2	Terminal 1	$\delta_1 = 3$	$(1,3)^T$	The main deviation occurs at Terminal 2
K3	Terminal 2	$\delta_2 = 4$	$(4,1)^T$	The main deviation occurs at Terminal 1

3.4 Normalization Related to Service-Time Delay

This section discusses normalization caused by service-time delay. In this context, the delay appears as an additional travel time or service time on a network component, so that the weight a_{ij} changes to $a_{ij} + d_{ij}$. Therefore, the disturbance analyzed here is not a delay in bus release from the terminal, but an increase in service duration on a local route or an interterminal corridor.

The system state is normalized with respect to the nominal period by

$$z(k) = x(k) - k\lambda\mathbf{1}. \tag{13}$$

Where $\mathbf{1}$ denotes the vector, whose entries are all 1 and the operation on equation (13) is standard addition and multiplication vector.

The system is said to return to the nominal phase if $z(k) = (0,0)^T$. The system is said to return to a periodic form if $z(k+c) = z(k)$ for some cyclicity c, although its phase may be shifted from the initial timetable. In this two-terminal network, the relevant cyclicity is $c = 2$. This distinction is important because the service may become mathematically repetitive again while still being late relative to the timetable announced to passengers.

For service delay, the excess delay on component $j \to i$ is expressed as

$$D_{ij}^L = max\{0, d_{ij} - \theta_{ij}\}. \tag{14}$$

If $D_{ij}^L = 0$, the additional service time is still absorbed by the available time buffer. If $D_{ij}^L > 0$, the deviation must be recovered so that the service phase returns closer to the nominal timetable.

For illustration, assume that the setup cost of fast mode is $c_s = 1$ equivalent minute and the recovery rate is $r = 4$ minutes per cycle. The initial excess delay D after m recovery cycles is estimated as

$$D(m) = max\{0, D - (mr - c_s)\}, \quad m = 1,2, \dots. \tag{15}$$

The system is considered recovered when $D(m) = 0$. This condition is equivalent to $D - (mr - c_s) \leq 0$ or $m \geq \frac{D+c_s}{r}$. We take the ceiling value since the number of recovery cycles must be an integer. Thus, the estimated minimum recovery horizon is

$$T_{\text{rec}}(D; r, c_s) = \left\lceil \frac{D + c_s}{r} \right\rceil. \tag{16}$$

This formula uses a one-time setup cost, whereas r is used as the recovery rate per cycle. The values of c_s and r in this article are illustrative and must be calibrated with field data before implementation.

Suppose that an additional service time occurs on the Terminal 1 local route with $d_{11} = 5$ minutes. Because the threshold of the Terminal 1 local route is $\theta_{11} = 2$ minutes, the excess service delay is

$$D_{11}^{L} = max\{0,5-2\} = 3. \tag{17}$$

With the illustrative parameters $c_s = 1$ and $r = 4$, the normalization time is estimated as

$$T_{\text{rec}}(3;4,1) = \left\lceil \frac{3+1}{4} \right\rceil = 1. \tag{18}$$

This means that one cycle of recovery mode is sufficient to eliminate the deviation caused by the local service delay, provided that the recovery rate is actually achieved in the field.

The next example occurs on the interterminal corridor from Terminal 1 to Terminal 2. If the service time on this corridor increases by $d_{21} = 2$ minutes, then $\theta_{21} = 0$ because the corridor is critical. Consequently,

$$D_{21}^{L} = max\{0,2-0\} = 2, \tag{19}$$

and

$$T_{\text{rec}}(2;4,1) = \left\lceil \frac{2+1}{4} \right\rceil = 1. \tag{20}$$

Although the illustrative normalization time is one cycle in both cases, the interpretation is different. On a local route, part of the delay is absorbed by the local threshold. On a critical corridor, the entire additional service time immediately becomes a deviation that must be recovered. Figure 2 shows the phase deviation caused by delay on a critical corridor.

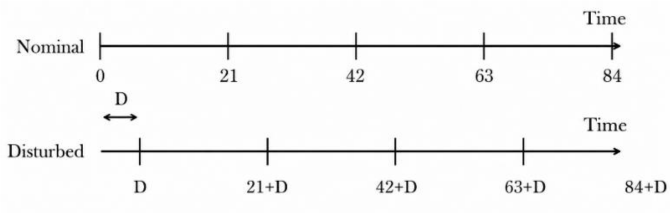

Figure 2. Illustration of phase deviation caused by service-time delay on a critical component.

3.5 Normalization Related to Departure-Time Delay

This section discusses normalization caused by departure-time delay. Unlike service delay, departure delay does not directly change the route weight. The disturbance appears because the departure event from terminal j is delayed by $\delta_j(k)$, so that the event time entering the next relation becomes $x_j(k) + \delta_j(k)$.

For departure-time delay, the excess delay on the relation departing from terminal j to terminal i is written as

$$D_{ij}^{B} = max\{0, \delta_j - \theta_{ij}\}. \tag{21}$$

Because one departure from a terminal may affect both a local route and an interterminal corridor, the normalization measure used by the operator can be taken as the maximum impact.

Table 6 shows the computation summary of the excess delay on equation (21) and minimum recovery horizon from equation (16).

Table 6. Numerical examples of departure-time delay normalization

Case	Departure disturbance	Delay δ	Smallest threshold	Excess D^B	T_{rec}
Departure-1	Terminal 1 delayed by 1 minute	1	0	1	1 cycle
Departure-2	Terminal 1 delayed by 3 minutes	3	0	3	1 cycle
Departure-3	Terminal 2 delayed by 4 minutes	4	0	4	2 cycles
Departure-4	Terminal 2 delayed by 8 minutes	8	0	8	3 cycles

The deviation trajectory for the departure-4 is presented in Table 7. With $D^B = 8$, $c_s = 1$ and $r = 4$, we have

$$T_{\text{rec}}(8;4,1) = \left\lceil \frac{8+1}{4} \right\rceil = 3.$$

If one service cycle is 21 minutes, then three cycles are equivalent to approximately 63 minutes of nominal operating time. This value is not the additional passenger waiting time, but the recovery horizon until the phase deviation returns to zero. The delay excess for each cycles determine using equation (15).
For cycle $m = 2$, we have.

$$D(2) = max\{0{,}8 - (8 - 1)\} = \max\{0{,}8 - 7\} = \max\{0{,}1\} = 1$$

The trajectory of delay excess for each cycle of m is showed in table 7.

Table 7. Normalization trajectory of Terminal 2 departure delay with $D^B = 8$, $c_s = 1$, and $r = 4$

Recovery cycle m	Value of D(m)	Status
0	8	Not yet recovered
1	5	Still delayed
2	1	Almost recovered
3	0	Back to normal

The above computation shows that departure-time delay may have a sharper impact than local service delay. The reason is that a departure from a terminal entering a critical corridor has a zero threshold. Therefore, normalization related to departure-time delay should be separated from normalization related to service delay so that the operator can distinguish the source of disturbance and select an appropriate recovery action.

3.6 Switching Policy Related to Service-Time Delay

The first switching policy addresses service-operational-time delay. For this type of disturbance, the operator observes the additional travel time or service time on a route and compares it with the threshold of each component. The excess service delay in cycle k is defined as

$$D^L(k) = \max_{(i,j)}\{max\big(0, d_{ij}(k) - \theta_{ij}\big)\}, \tag{22}$$

where $d_{ij}(k)$ denotes the additional service time on component $j \to i$. Parameter r denotes the reduction of deviation per cycle after fast mode is activated, c_s denotes the one-time setup cost, H denotes the predictive horizon, and h_{on} and h_{off} denote activation and deactivation hysteresis. The net benefit of fast mode over the H-cycle horizon is

$$B_H = Hr - c_s. \tag{23}$$

For service-time delay, fast mode is recommended if

$$D^L(k) \geq c_s + h_{\text{on}}, \quad Hr - c_s \geq D^L(k) + h_{\text{on}}. \tag{24}$$

The system returns to normal mode if

$$D^L(k) \leq h_{\text{off}}, \quad 0 \leq h_{\text{off}} < h_{\text{on}}. \tag{25}$$

Take the illustrative parameters $c_s = 1$, $r = 4$, $H = 2$, $h_{on} = 1$, and $h_{off} = 0.5$. If the Terminal 1 local route is delayed by $d = 5$ minutes, then Equation (9) gives $D^L = 3$. Because

$$\begin{aligned} &D^L = 3 \geq c_s + h_{\text{on}} = 2, \\ &Hr - c_s = 2(4) - 1 = 7 \geq D^L + h_{\text{on}} = 4. \end{aligned} \tag{26}$$

fast mode is feasible to activate. In the service context, fast mode may include reducing waiting time at internal stops, prioritizing terminal exit, using a smoother route where available, or dispatching a spare bus to maintain the next cycle.

Table 8. Examples of switching decisions for service-time delay

Case	Service disturbance	D^L	Activation condition	Decision
L1	Terminal 1 local route delayed by 1 minute	0	Not satisfied	Normal mode
L2	Terminal 1 local route delayed by 5 minutes	3	Satisfied	Fast mode/active recovery
L3	Terminal 2 local route delayed by 5 minutes	2	Satisfies the activation threshold	Limited fast mode or active recovery
L4	Terminal 1 to Terminal 2 corridor delayed by 2 minutes	2	Satisfies the activation threshold	Limited fast mode or corridor priority

3.7 Switching Policy Related to Departure-Time Delay

The second switching policy addresses departure-time delay. For this type of disturbance, the operator considers not only the length of additional travel time but also the delay in bus release from the terminal. The excess departure delay in cycle k can be written as

$$D^B(k) = \max_{(i,j)}\{max(0, \delta_j(k) - \theta_{ij})\}, \tag{27}$$

where $\delta_j(k)$ denotes the departure delay from terminal j. Since one departure from a terminal may affect more than one relation, the maximum value in Equation (27) is used to capture the worst impact in that cycle.
Fast mode for departure-time delay is recommended if

$$D^B(k) \geq c_s + h_{\text{on}}, \quad Hr - c_s \geq D^B(k) + h_{\text{on}}. \tag{28}$$

The system returns to normal mode if

$$D^B(k) \leq h_{\text{off}}. \tag{29}$$

The main difference from service delay lies in the form of intervention. For departure-time delay, the intervention may include releasing a replacement bus, accelerating boarding and alighting before the next scheduled departure, limiting terminal waiting time, or rearranging the departure sequence.

Given the following numerical example of the switching policy for departure-time delay. Use the same parameters, namely $c_s = 1, r = 4, H = 2, h_{on} = 1$, and $h_{\text{off}} = 0.5$. If Terminal 1 is delayed in departure by $\delta_1 = 1$ minute, then on the critical relation from Terminal 1 to Terminal 2 we obtain $D^B = 1$. Since $1 < c_s + h_{on} = 2$, the system does not need to enter fast mode; local recovery, such as accelerating terminal processes in the next cycle, is sufficient. Table 9 gives some cases of departure-delay that affect to the switching decision.

Table 9. Examples of switching decisions for departure-time delay

Case	Departure disturbance	D^B	Activation condition	Decision
B1	Terminal 1 delayed by 1 minute	1	Not satisfied	Local recovery
B2	Terminal 1 delayed by 3 minutes	3	Satisfied	Fast mode/departure resequencing
B3	Terminal 2 delayed by 4 minutes	4	Satisfied	Fast mode or replacement bus

A small sensitivity sweep was conducted to illustrate how the recovery horizon changes when the excess delay D, setup cost c_s, and recovery rate r are varied. The recovery horizon was computed using equation (16)

Table 10. Sensitivity of recovery horizon to excess delay, setup cost, and recovery rate

Excess delay (D)	Setup cost (c_s)	Recovery rate (r)	T_{rec}	Interpretation
2	1	4	1 cycle	Small disturbance is recovered quickly
4	1	4	2 cycles	Moderate delay requires longer recovery
8	1	4	3 cycles	Baseline case used in Table 7
8	0	4	2 cycles	Lower setup cost shortens recovery
8	2	4	3 cycles	Higher setup cost may keep the same rounded horizon
8	1	2	5 cycles	Lower recovery rate strongly increases recovery time
8	1	6	2 cycles	Higher recovery rate shortens recovery time

The sweep shows that T_{rec} is more sensitive to the recovery rate r than to small changes in setup cost c_s, especially for larger excess delays. Therefore, field calibration of r is essential before the switching rule is used operationally. The predictive horizon H and hysteresis parameters h_{on} and h_{off} should also be chosen conservatively when delay magnitude d or departure delay δ is highly variable.

If service delay and departure-time delay occur simultaneously in a cycle, the operator may use the combined indicator

$$D(k) = max\{D^L(k), D^B(k)\}. \tag{30}$$

This indicator ensures that the switching decision follows the dominant disturbance. Thus, the operational rule remains simple while still distinguishing the source of delay and the corresponding recovery action.

3.8 Discussion

The computational results show that the two-terminal TGMEB network has a simple but strict synchronization structure. The nominal period is determined by the critical interterminal corridors, not by the local terminal loops. This means that delay management in the network should not treat all route components equally. Local-route disturbances can be tolerated up to their thresholds, whereas disturbances on the interterminal corridors immediately affect the synchronized timetable. From a max-plus perspective, this result follows from the position of the critical arcs in the weighted directed graph. From an operational perspective, it implies that monitoring and recovery should prioritize interterminal departures and arrivals.

The contribution of this study differs from both general max-plus scheduling studies and electric-bus optimization studies. Max-plus scheduling studies usually emphasize timetable construction, compression, or system representation [6–8]. Max-plus control studies provide broader frameworks for optimization, uncertainty, and switched-system analysis [9, 11, 12]. In contrast, this article focuses on delay thresholds and excess-delay indicators in a small synchronized network. Electric-bus optimization studies usually emphasize fleet assignment, charging decisions, charging-station capacity, and energy feasibility [16–18]. The present study examines how a delay in a specific route component changes the synchronization state of the system. Therefore, the novelty lies in connecting max-plus criticality, component-wise delay tolerance, normalization time, and a recovery switching rule within one analytical framework.

The proposed switching rule should be interpreted as an initial analytical heuristic rather than a fully optimized control strategy. Its parameters, such as setup cost, recovery rate, predictive horizon, and hysteresis margin, were introduced to illustrate how mathematical excess-delay indicators can be translated into operational decisions. These parameters have not yet been calibrated using field observations. The study also does not include GPS-based travel-time records, observed departure delays, passenger-demand variation, charging logs, or stochastic energy-consumption data. The recovery decisions in table 8 and 9 are analytical decision rules derived from the max-plus structure of the nominal network. Therefore, the framework is best understood as a deterministic max-plus baseline model. Future studies should extend it by using empirical data, stochastic delay distributions, and simulation-based validation.

For operational calibration, future TGMEB data collection should include timestamped departures and arrivals at each terminal, GPS-based travel times for local and interterminal routes, dwell times at stops and terminals, charging-related delay logs, passenger boarding patterns, and records of replacement-bus or priority-dispatch actions. A minimum observation period of two to four weeks is recommended to capture weekday-weekend differences, peak and off-peak patterns, weather effects, and day-to-day variability. These data would allow the parameters c_s, r, H, h_{on}, and h_{off} to be estimated empirically rather than treated as illustrative values.

4. CONCLUSION

This study analyzed delay tolerance, normalization time, and recovery switching in the two-terminal TGMEB network using max-plus algebra. The nominal network was represented as a weighted directed graph and transformed into a max-plus linear system. The max-plus eigenvalue showed that the synchronized service period was 21 minutes. The local routes at Terminal 1 and Terminal 2 had delay thresholds of 2 and 3 minutes, respectively, whereas the two interterminal corridors were critical arcs with zero delay tolerance. Therefore, any positive delay on an interterminal corridor directly disturbed the synchronized timetable.

The analysis also showed that service-operational delay and departure-time delay must be distinguished because they enter the model differently. Service-operational delay changes the route weight, whereas departure-time delay shifts the terminal event time. In both cases, the excess-delay indicator determines whether a disturbance can still be absorbed or must be recovered. This indicator provides the mathematical basis for estimating normalization time and for distinguishing normal operation, local recovery, and fast-mode recovery.

The principal mathematical contribution of this study is a deterministic max-plus framework that links critical arcs, delay thresholds, excess delay, normalization horizons, and recovery switching in a small synchronized electric-bus network. Practically, the framework suggests that TGMEB operators should prioritize the monitoring and recovery of interterminal corridors, while local-route delays may be tolerated as long as they remain within the computed thresholds. Future research should validate the proposed framework using actual operational data, including departure times, travel times, charging-related delays, passenger demand, and stochastic delay patterns.

ACKNOWLEDGEMENT

The authors gratefully acknowledge the financial support provided by the Institute for Research and Community Service of Sanata Dharma University. Funding for this research through the Basic Research Scheme with Contract No.: 009 Penel./LPPM-USD/II/2026.

5. REFERENCES

[1] F. B. Pranatta, M. A. Rudhito, and D. P. W. Putra, "Designing an Optimal Route Network for the Synchronized Trans Gadjah Mada Electric Bus (TGMEB) using Max-Plus Algebra," *ZERO: Jurnal Sains, Matematika dan Terapan*, vol. 9, no. 2, p. 335, 2025. [Online]. Available: https://doi.org/10.30829/zero.v9i2.25392

[2] F. Baccelli, G. Cohen, G. J. Olsder, and J.-P. Quadrat, *Synchronization and Linearity: An Algebra for Discrete Event Systems*, Paris, France, Wiley, 2001.

[3] B. Heidergott, G. J. Olsder, and J. van der Woude, *Max Plus at Work*, Princeton, NJ, USA, Princeton University Press, 2006.

[4] M. A. Rudhito, *Aljabar Max-Plus dan Penerapannya*, Yogyakarta, Indonesia, Sanata Dharma University Press, 2016.

[5] C. G. Cassandras and S. Lafortune, *Introduction to Discrete Event Systems*, New York, NY, USA, Springer, 2008. [Online]. Available: https://doi.org/10.1007/978-0-387-68612-7

[6] J. Uyttendaele, I. Van Hoeck, N. Besinovic, and P. Vansteenwegen, "Timetable compression using max-plus automata applied to large railway networks," *TOP*, vol. 31, no. 2, pp. 414–439, 2023. [Online]. Available: https://doi.org/10.1007/s11750-022-00641-5

[7] E. Carnia, R. Wilopo, H. Napitupulu, N. Anggriani, and A. K. Supriatna, "Modified Kleene Star Algorithm Using Max-Plus Algebra and Its Application in the Railroad Scheduling Graphical User Interface," *Computation*, vol. 11, no. 1, p. 11, 2023. [Online]. Available: https://doi.org/10.3390/computation11010011

[8] V. Eramo, T. Fiori, F. G. Lavacca, and F. Valente, "A max plus algebra based scheduling algorithm for supporting time triggered services in Ethernet networks," *Computer Communications*, vol. 198, pp. 85–97, 2023. [Online]. Available: https://doi.org/10.1016/j.comcom.2022.11.014

[9] C. Wang and Y. Tao, "Locally and globally optimal solutions of global optimisation for max-plus linear systems," *IET Control Theory & Applications*, vol. 16, no. 2, pp. 219–228, 2022. [Online]. Available: https://doi.org/10.1049/cth2.12219

[10] C. Wang, Y. Xia, Z. Li, and Y. Tao, "Approximately global optimal control for max-plus linear systems and its application on load distribution," *International Journal of Control*, vol. 96, no. 5, pp. 1104–1115, 2023. [Online]. Available: https://doi.org/10.1080/00207179.2022.2031301

[11] C. Wang, Y. Song, Y. Wang, and Z. Li, "Bi-Objective Optimization for Interval Max-Plus Linear Systems," *Mathematics*, vol. 12, no. 5, p. 653, 2024. [Online]. Available: https://doi.org/10.3390/math12050653

[12] D. Zorzenon, J. Komenda, and J. Raisch, "Switched max-plus linear-dual inequalities: cycle time analysis and applications," *Discrete Event Dynamic Systems*, vol. 34, no. 1, pp. 199–250, 2024. [Online]. Available: https://doi.org/10.1007/s10626-023-00389-5

[13] H. Al Bermanei, J. M. Böling, and G. Högnäs, "Modeling and scheduling of production systems by using max-plus algebra," *Flexible Services and Manufacturing Journal*, vol. 36, no. 1, pp. 129–150, 2024. [Online]. Available: https://doi.org/10.1007/s10696-023-09484-z

[14] S. S. G. Perumal, R. M. Lusby, and J. Larsen, "Electric bus planning & scheduling: A review of related problems and methodologies," *European Journal of Operational Research*, vol. 301, no. 2, pp. 395–413, 2022. [Online]. Available: https://doi.org/10.1016/j.ejor.2021.10.058

[15] L. Zhang, Y. Han, J. Peng, and Y. Wang, "Vehicle and charging scheduling of electric bus fleets: A comprehensive review," *Journal of Intelligent and Connected Vehicles*, vol. 6, no. 3, pp. 116–124, 2023. [Online]. Available: https://doi.org/10.26599/JICV.2023.9210012

[16] Y. Bie, J. Ji, X. Wang, and X. Qu, "Optimization of electric bus scheduling considering stochastic volatilities in trip travel time and energy consumption," *Computer-Aided Civil and Infrastructure Engineering*, vol. 36, no. 12, pp. 1530–1548, 2021. [Online]. Available: https://doi.org/10.1111/mice.12684

[17] M. H. de Vos, R. N. van Lieshout, and T. Dollevoet, "Electric Vehicle Scheduling in Public Transit with Capacitated Charging Stations," *Transportation Science*, vol. 58, no. 2, pp. 279–294, 2024. [Online]. Available: https://doi.org/10.1287/trsc.2022.0253

[18] M. Duan, F. Liao, G. Qi, and W. Guan, "Integrated optimization of electric bus scheduling and charging planning incorporating flexible charging and timetable shifting strategies," *Transportation Research Part C: Emerging Technologies*, vol. 152, p. 104175, 2023. [Online]. Available: https://doi.org/10.1016/j.trc.2023.104175

[19] J. He, N. Yan, J. Zhang, Y. Yu, and T. Wang, "Battery electric buses charging schedule optimization considering time-of-use electricity price," *Journal of Intelligent and Connected Vehicles*, vol. 5, no. 2, pp. 138–145, 2022. [Online]. Available: https://doi.org/10.1108/JICV-03-2022-0006

[20] Y. Liu, L. Wang, Z. Zeng, and Y. Bie, "Optimal charging plan for electric bus considering time-of-day electricity tariff," *Journal of Intelligent and Connected Vehicles*, vol. 5, no. 2, pp. 123–137, 2022. [Online]. Available: https://doi.org/10.1108/JICV-04-2022-0008

[21] M. L. Y. Chau, D. Koutsompina, and K. Gkiotsalitis, "The Electric Vehicle Scheduling Problem for Buses in Networks with Multi-Port Charging Stations," *Sustainability*, vol. 16, no. 3, p. 1305, 2024. [Online]. Available: https://doi.org/10.3390/su16031305

[22] D. McCabe, X. Ban, and B. Kulcsár, "Minimum-delay opportunity charging scheduling for electric buses," *Communications in Transportation Research*, vol. 5, p. 100209, 2025. [Online]. Available: https://doi.org/10.1016/j.commtr.2025.100209

[23] L. Zhang, Y. Wang, W. Gu, Y. Han, E. Chung, and X. Qu, "On the role of time-of-use electricity price in charge scheduling for electric bus fleets," *Computer-Aided Civil and Infrastructure Engineering*, vol. 39, no. 8, pp. 1218–1237, 2024. [Online]. Available: https://doi.org/10.1111/mice.13134

[24] M. Zhang, M. Yang, Y. Li, and S. Huang, "Optimization of Electric Bus Scheduling Considering Charging Station Resource Constraints," *Transportation Research Record*, vol. 2678, no. 3, pp. 13–23, 2024. [Online]. Available: https://doi.org/10.1177/03611981231178307

[25] Y. Xing, Q. Fu, Y. Li, H. Chu, and E. Niu, "Optimal Model of Electric Bus Scheduling Based on Energy Consumption and Battery Loss," *Sustainability*, vol. 15, no. 12, p. 9640, 2023. [Online]. Available: https://doi.org/10.3390/su15129640

[26] Y. Liu, B. Zeng, K. Long, and W. Wu, "Enhancing Electric Bus Charging Scheduling: An Energy-Integrated Dynamic Bus Replacement Strategy with Time-of-Use Pricing," *Sustainability*, vol. 16, no. 8, p. 3334, 2024. [Online]. Available: https://doi.org/10.3390/su16083334

[27] L. S. Ashkezari, H. J. Kaleybar, and M. Brenna, "Electric Bus Charging Infrastructures: Technologies, Standards, and Configurations," *IEEE Access*, vol. 12, pp. 80505–80528, 2024. [Online]. Available: https://doi.org/10.1109/ACCESS.2024.3410880

[28] L. Zhong, Z. Zeng, Z. Huang, X. Shi, and Y. Bie, "Joint optimization of electric bus charging and energy storage system scheduling," *Frontiers of Engineering Management*, vol. 11, no. 4, pp. 676–696, 2024. [Online]. Available: https://doi.org/10.1007/s42524-024-3102-2

[29] H. Hu, B. Du, W. Liu, and P. Perez, "A joint optimisation model for charger locating and electric bus charging scheduling considering opportunity fast charging and uncertainties," *Transportation Research Part C: Emerging Technologies*, vol. 141, p. 103732, 2022. [Online]. Available: https://doi.org/10.1016/j.trc.2022.103732

[30] L. Li, H. K. Lo, W. Huang, and F. Xiao, "Mixed bus fleet location-routing-scheduling under range uncertainty," *Transportation Research Part B: Methodological*, vol. 146, pp. 155–179, 2021. [Online]. Available: https://doi.org/10.1016/j.trb.2021.02.009